Rényi holographic dark energy (RHDE) in Lyra Geometry

Jumi Bharali[1], Kanika Das[2]
[1,2]Department of Mathematics, Gauhati University, Assam (India)
[1]jumibharali2@gmail.com,[2]kallol@gauhati.ac.in
(Submitted on 20.06.2021; Accepted on 08.08.2021)

Abstract. In this proposed problem we study Rényi Holographic Dark Energy (RHDE) models by considering a spatially homogenous and anisotropic Bianchi type V space-time with bulk viscosity in Lyra's manifold with time-dependent displacement field. The exact solutions of the field equations have been found for a Bianchi type V space-time in Lyra's geometry by considering a time-dependent displacement field. We have discussed two different types of models: non-interacting and interacting ones. Remarkably, at late times the EOS parameter for the non-interacting model corresponds to quintessence DE, whereas for the interacting model it corresponds to phantom DE showing consistency with the recent observational data. The study of statefinder parameters shows that our RHDE model corresponds to ΛCDM (cosmological constant cold dark matter) model at the later stage of the Universe. The correspondence between the non-interacting model and a quintessence scalar field and also the correspondence between the interacting model and a phantom scalar field are also established. A detailed study of physical and geometric properties of both the non-interacting and interacting models has been carried out.
Key words: RHDE, bulk viscosity, Lyra Geometry, EOS parameter, phantom DE, quintessence DE

Introduction

Observations, investigated by a considerable number of researchers in refs. (Riess et al. [1998], Perlmutter et al. [1998], Bennett et al. [2003], Spergel et al. [2003], Tegmark et al. [2004], Page et al. [2003]), confirmed that our Universe is undergoing an accelerated phase of expansion. All these findings demonstrate that our Universe is dominated by an exotic form of energy named as dark energy (DE). DE, which is responsible for cosmic acceleration, is still unknown. DE has negative pressure, so is repulsive and causes the expansion of the Universe. Again, the astronomical observations suggest that our Universe comprises of 68.3% in the form of DE, 26.8% DM (dark matter, non-baryonic) and the rest 4.9% is baryonic matter and radiation Ade, [2013]. There are numerous candidates for DE such as the cosmological constant or vacuum energy, originally introduced by Einstein, quintessence $\left(-1 < \omega < \frac{-1}{3}\right)$ in ref. Sami and Padmanabhan [2003], phantom ($\omega < -1$) in ref. Caldwell et al. [2003], k-essence $\left(\omega < \frac{-1}{3}\right)$ in ref. Chiba [2002], Chaplygin gas in ref. Kamenshchik et al. [2001], etc. The cosmological constant $\Lambda(\omega = -1)$ is the simplest and the most usual candidate for DE and the ΛCDM model is a quite successful model. But this proposition contains several difficulties as the fine-tuning and cosmic coincidence problem in refs. Weinberg [1989], Overduin and Cooperstock [1998]. Carroll et al. [2003] derived a DE model in which DE is considered as a fluid by the EOS parameter $\omega = \frac{p}{\rho}$, which is not necessarily constant and where p is the pressure and ρ is the energy density of DE. We become interested to investigate ω throughout the evolution of the Universe.

The holographic dark energy (HDE), based on the holographic principle, was first put forward by Hooft [1993] and Susskind [1995]. According to this

principle, the entropy of the system scales not with its volume, but also its surface area $\left(L^2\right)$ and leads to the conclusion that in quantum field theory a short distance cut-off is related to a long-distance cut-off due to the limit set by the black hole formation (ref. Cohen et al. [1999]). By taking ρ_{HDE} as the quantum zero-point energy density caused by a short distance cut-off in a region of size L, the total energy density should not exceed the black hole mass of the same size, giving $L^3\rho_{HDE} \leq LM_p^2$. The maximal value L allowed is the one saturating this inequality, giving the HDE density as $\rho_{HDE} = 3c^2M_p^2L^{-2}$, M_p is the reduced Planck mass with $M_p^{-2} = 8\pi G$, and $3c^2$ is the numerical constant (ref. Li [2004]).

The form of the Bekenstein entropy of a system is $S = \frac{A}{4}$, where $A = 4\pi L^2$, and L is the IR cut-off. R*é*nyi entropy (ref. Moradpour et al. [2018]) can be written as $S = \frac{1}{\delta}\log\left(\frac{\delta A}{4} + 1\right) = \frac{1}{\delta}\log\left(\pi\delta L^2 + 1\right)$. By considering $\rho_{DE}dV \propto TdS$, where V and T denote the volume and temperature of the system, respectively, the expression of RHDE assumes the form $\rho_{DE} = \frac{3c^2}{8\pi L^2}\left(\pi\delta L^2 + 1\right)^{-1}$. By considering Hubble horizon as a candidate for IR cut-off, i.e. $L = H^{-1}$, the energy density of RHDE is obtained as $\rho_{DE} = \frac{3c^2H^2}{8\pi\left(\frac{\pi\delta}{H^2}+1\right)}$, where c^2 is a numerical constant.

The Hubble parameter H describes the expansion rate of the Universe, and the deceleration parameter q signifies the accelerating and decelerating nature of the Universe. On the basis of the time dependence of H and q, various models of the Universe can be classified. All models can be characterized by whether they expand or contract, and accelerate or decelerate (in ref. Bolotin et al. [2015]). Following Tiwari et al. [2018], [2017], [2017], [2016], we have considered q as a simple linear function of H, i.e. $q = \mu + \nu H$, where μ and ν are constants. For mathematical simplicity, we take $\mu = -1$, which in turn implies $q = -1 + \nu H$.

The appearance of bulk viscosity in the early Universe plays a great role. When neutrons decouple from the cosmic fluid at the time of formation of galaxies and during particle creation in the early Universe, viscosity arises (ref. Misner [1968]). It is essential to mention that the presence of viscosity in the fluid explores many dynamics in the framework of homogenous cosmological models. The coefficient of bulk viscosity yields the viscous stress magnitude relative to the expansion. In an attempt to study the early evolution of the Universe, considerable number of authors have investigated cosmological dynamics, with a fluid containing viscosity by Singh [2008], Singh and Srivastava [2018], Pradhan et al. [2007]. The viscosity mechanisms in cosmology can account for the high entropy of the present Universe (refs. Weinberg [1971] and Weinberg [1972]). The coefficient of viscosity decreases as the Universe expands. Padmanabhan and Chitre [1987] found that the presence of bulk viscosity leads to inflationary-like solutions in general relativity (GR). Meng and Ma [2012] studied singularity free bulk viscous cosmological models by considering the bulk viscous coefficient as a linear and quadratic functions of the Hubble parameter H. The concept of bulk viscosity ζ introduces dissipation by only redefining the effective pressure $\bar{p}$, where $\bar{p} = p - 3\zeta H$.

Several researchers were inspired by Einstein's geometrization of gravitation in his theory of general relativity to geometrize other physical fields. Weyl [1918] proposed a unified theory to geometrize gravitation and electromagnetism. But this theory was not considered as it was depended on non-integrability of length transfer. Lyra [1951] proposed a new modification of Riemannian geometry by introducing a gauge function to remove the non-integrability of the length of a vector under parallel transport. Sen [1957] and Sen and Dunn [1971] suggested a new scalar-tensor theory of gravitation and constructed an analogue of the Einstein field equations based on Lyra's geometry, which in normal gauge may be written as
$R_{ij} - \frac{1}{2}g_{ij}R + \frac{3}{2}\phi_i\phi_j - \frac{3}{4}g_{ij}\phi_k\phi^k = -T_{ij}$,
where ϕ_i is the displacement vector, $8\pi G = 1$ and other symbols have their usual meaning in the Riemannian Geometry.

Recently, various cosmological models in Lyra geometry were studied by considerable number of researchers. Pradhan and Pandey [2003] have obtained bulk viscous cosmological models in Lyra geometry. Kandalkar and Samdurkar [2015] have studied LRS Bianchi type I metric with bulk viscosity in the framework of Lyra geometry. Pradhan et al. [2001] have discussed FRW spacetime in the presence of a bulk viscous fluid in Lyra manifold. Sharma and Dubey [2020] have investigated interacting RHDE in a flat FRW Universe. Prasanthi and Aditya [2020] have worked out anisotropic Bianchi type-VI_0 RHDE models in general relativity (GR). Bhattacharjee [2020] have presented Tsallis and RHDE with hybrid expansion law prescribed by a non-linear interaction in the FRW spacetime. Bianchi type Universes play a significant role in the description of large-scale behaviour of the Universe. Bianchi models are important due to the homogeneity and anisotropic nature. Due to its simplicity, several researchers have studied them in different frameworks. In this paper, we have examined the RHDE model by considering Bianchi type V space-time with bulk viscosity in Lyra's geometry with time-dependent displacement field.

The plan of the paper is as follows. In Section 2, we present the metric and the field equations. The solutions of the field equations are described in Section 3. Section 4 deals with non-interacting model, followed by subsections 4.1 - energy conditions and 4.2 - correspondence between non-interacting model and quintessence scalar field model are established. Section 5 is concerned with interacting model, followed by subsections 5.1 - energy conditions of the interacting model, and 5.2 deals with correspondence between interacting model and phantom scalar field model. Section 6 deals with graphical representations of various parameters. Cosmic jerk, Statefinder and Anisotropy parameters are discussed in Sections 7, 8 and 9, respectively. The paper ends with concluding remarks in Section 10.

2. Metric and Field Equations

Einstein field equations, based on Lyra manifold in normal gauge are written as

$$R_{ij} - \frac{1}{2}g_{ij}R + \frac{3}{2}\phi_i\phi_j - \frac{3}{4}g_{ij}\phi_k\phi^k = -T_{ij}, \tag{1}$$

where ϕ_i is the displacement vector, $8\pi G = 1$ and other symbols have their usual meaning in the Riemannian Geometry.

$$T_{ij} = \bar{T}_{ij} + T'_{ij}, \tag{2}$$

where $\bar{T}_{ij} = \rho_m u_i u_j$ is the energy momentum tensor for dark matter (pressure-less), ρ_m is the energy density of dark matter (DM), $g_{ij}u^i u^j = 1$, $u^j = (1, 0, 0, 0)$ is the four-velocity vector. $T'_{ij} = (\bar{p}_{de} + \rho_{de})\, u_i u_j - \bar{p}_{de} g_{ij}$ is the energy momentum tensor for RHDE, where $\bar{p}_{de} = p_{de} - 3H\zeta$ is the effective pressure of RHDE, ρ_{de} is the energy density and p_{de} is the pressure of RHDE. The displacement vector ϕ_i is defined as

$$\phi_i = (\beta\,(t)\,, 0, 0, 0))\,. \tag{3}$$

We consider the Bianchi type V space-time in the form

$$ds^2 = dt^2 - E^2 dx^2 - e^{2x}\left(F^2 dy^2 + G^2 dz^2\right), \tag{4}$$

where E, F and G are cosmic scale factors and functions of cosmic time t only. The field equations (1) for the metric (4), with the use of Eqs. (2) and (3) reduce to the following

$$\frac{\ddot{F}}{F} + \frac{\ddot{G}}{G} + \frac{\dot{F}\dot{G}}{FG} - \frac{1}{E^2} + \frac{3}{4}\beta^2 = -p_{de} + 3H\zeta, \tag{5}$$

$$\frac{\ddot{E}}{E} + \frac{\ddot{G}}{G} + \frac{\dot{E}\dot{G}}{EG} - \frac{1}{E^2} + \frac{3}{4}\beta^2 = -p_{de} + 3H\zeta, \tag{6}$$

$$\frac{\ddot{E}}{E} + \frac{\ddot{F}}{F} + \frac{\dot{E}\dot{F}}{EF} - \frac{1}{E^2} + \frac{3}{4}\beta^2 = -p_{de} + 3H\zeta, \tag{7}$$

$$\frac{\dot{E}\dot{F}}{EF} + \frac{\dot{F}\dot{G}}{FG} + \frac{\dot{E}\dot{G}}{EG} - \frac{3}{E^2} - \frac{3}{4}\beta^2 = \rho_m + \rho_{de}, \tag{8}$$

$$2\frac{\dot{E}}{E} - \frac{\dot{F}}{F} - \frac{\dot{G}}{G} = 0, \tag{9}$$

where overhead dot (.) stands for derivative with respect to time t.
The energy conservation equation is

$$\dot{\rho}_m + \left(\frac{\dot{E}}{E} + \frac{\dot{F}}{F} + \frac{\dot{G}}{G}\right)\rho_m + \dot{\rho}_{de} + (1 + \omega_{de})\left(\frac{\dot{E}}{E} + \frac{\dot{F}}{F} + \frac{\dot{G}}{G}\right)\rho_{de} + \frac{3}{2}\beta\dot{\beta} + \frac{3}{2}\beta^2\left(\frac{\dot{E}}{E} + \frac{\dot{F}}{F} + \frac{\dot{G}}{G}\right) - 9H^2\zeta = 0. \tag{10}$$

The continuity equations for DM and DE, where the DM component is interacting with the DE component through an interaction term Q, are termed as

$$\dot{\rho}_m + 3H\rho_m = 9H^2\zeta + Q, \tag{11}$$

$$\dot{\rho}_{de} + 3H\left(1 + \omega_{de}\right)\rho_{de} = -Q, \tag{12}$$

where $\omega_{de} = \frac{p_{de}}{\rho_{de}}$ is the equation of state parameter for RHDE, Q denotes the strength of the interaction. We have taken $Q = 3bH\rho_{de}$, with b as dimensionless constant (in ref. Wei and Cai [2009]). $Q = 0$ indicates the non-interacting scenario.

3. Solution of field equations

The average scale factor a and spatial volume V are defined as

$$V = a^3 = EFG. \tag{13}$$

Integrating Eq. (9) and taking the integration constant to be equal to unity we obtain

$$E^2 = FG. \tag{14}$$

The directional and the average Hubble parameter are defined as

$$H_x = \frac{\dot{E}}{E}, H_y = \frac{\dot{F}}{F}, H_z = \frac{\dot{G}}{G}, H = \frac{\dot{a}}{a} = \frac{\dot{V}}{3V} = \frac{H_x+H_y+H_z}{3} = \frac{1}{3}\left(\frac{\dot{E}}{E} + \frac{\dot{F}}{F} + \frac{\dot{G}}{G}\right) \tag{15}$$

where H_x, H_y and H_z are the directional Hubble parameters in the directions x, y and z, respectively.

The deceleration parameter q is defined as

$$q = \frac{-\ddot{a}}{aH^2}. \tag{16}$$

The expansion scalar θ and the shear scalar σ are defined as

$$\theta = u^i_{;i} = \frac{\dot{E}}{E} + \frac{\dot{F}}{F} + \frac{\dot{G}}{G}, \tag{17}$$

$$\sigma^2 = \frac{1}{2}\left(\sum_{i=1}^{3} H_i^2 - \frac{\theta^2}{3}\right) = \frac{1}{3}\left(\frac{\dot{E}^2}{E^2} + \frac{\dot{F}^2}{F^2} + \frac{\dot{G}^2}{G^2} - \frac{\dot{E}\dot{F}}{EF} - \frac{\dot{F}\dot{G}}{FG} - \frac{\dot{G}\dot{E}}{GE}\right). \tag{18}$$

To solve the field equations, we follow the technique of Saha and Rikhvitsky [2006], Singh and Chaubey [2007]. From Eqs. (5), (6) and (7), we get

$$\frac{E}{F} = e_1 exp\left(f_1 \int \frac{dt}{a^3}\right), \tag{19}$$

$$\frac{F}{G} = e_2 exp\left(f_2 \int \frac{dt}{a^3}\right), \tag{20}$$

$$\frac{G}{E} = e_3 exp\left(f_3 \int \frac{dt}{a^3}\right), \tag{21}$$

where e_1, e_2, e_3, f_1, f_2 and f_3 are constants of integration satisfying $e_1 e_2 e_3 = 1, f_1 + f_2 + f_3 = 0$.

From Eqs. (19)-(21), the metric coefficients are obtained as

$$E = g_1 a exp\left(\frac{F_1}{3} \int \frac{dt}{a^3}\right), \tag{22}$$

$$F = g_2 a exp\left(\frac{F_2}{3} \int \frac{dt}{a^3}\right), \tag{23}$$

$$G = g_3 a exp\left(\frac{F_3}{3} \int \frac{dt}{a^3}\right), \tag{24}$$

with
$g_1 = \left(\frac{e_1}{e_3}\right)^{\frac{1}{3}}, F_1 = f_1 - f_3, g_2 = \left(\frac{1}{e_1^2 e_3}\right)^{\frac{1}{3}}, F_2 = -2f_1 - f_3, g_3 = \left(e_1 e_3^2\right)^{\frac{1}{3}}, F_3 = f_1 + 2f_3$
Using Eqs. (22)-(24) in Eq. (14) we get:

$$g_1 = 1, g_2 = M^{-1}, g_3 = M, \tag{25}$$

$$F_1 = 0, F_2 = -K, F_3 = K. \tag{26}$$

With Eqs. (25) and (26), Eqs. (22)-(24) becomes

$$E = a, \tag{27}$$

$$F = aM^{-1} exp\left(\frac{-K}{3} \int \frac{dt}{a^3}\right), \tag{28}$$

$$G = aM exp\left(\frac{K}{3} \int \frac{dt}{a^3}\right). \tag{29}$$

Eqs. (5)-(8) and (10) can be written in terms of H, σ and q as

$$p_{de} - 3H\zeta = (2q - 1) H^2 - \sigma^2 + \frac{1}{a^2} - \frac{3}{4}\beta^2 \tag{30}$$

and

$$\rho_m + \rho_{de} = 3H^2 - \sigma^2 - \frac{3}{a^2} + \frac{3}{4}\beta^2 \tag{31}$$

Eqs. (30) and (31) are two field equations with four unknowns: a, ρ_m, ρ_{de} and β. To solve the system of field equations completely, we are in search of two extra relations:
(i) The RHDE density is defined as by Moradpour et al. [2018]:

$$\rho_{de} = \frac{3c^2H^2}{8\pi\left(\frac{\pi\delta}{H^2} + 1\right)} \tag{32}$$

(ii) The deceleration parameter q is considered as a linear function of the Hubble parameter H as by Tiwari et al. [2018], [2017], [2017], [2016]:

$$q = -1 + \nu H \tag{33}$$

From Eqs. (16) and (33), we get the expression of average scale factor a as

$$a = exp\left(\frac{1}{\nu}\sqrt{2\nu t + k}\right), \tag{34}$$

where ν and k are constants.

Using Eq. (34) in Eqs. (27)-(29), we get the following expressions of cosmic scale factors:

$$E = exp\left(\frac{1}{\nu}\sqrt{2\nu t + k}\right), \tag{35}$$

$$F = exp\left(\frac{1}{\nu}\sqrt{2\nu t + k}\right) M^{-1} exp\left[\frac{-K}{3}\int \frac{dt}{exp\left(\frac{3}{\nu}\sqrt{2\nu t + k}\right)}\right], \tag{36}$$

$$G = exp\left(\frac{1}{\nu}\sqrt{2\nu t + k}\right) M exp\left[\frac{K}{3}\int \frac{dt}{exp\left(\frac{3}{\nu}\sqrt{2\nu t + k}\right)}\right]. \tag{37}$$

The Hubble parameter H is calculated as

$$H = \frac{\dot{a}}{a} = \frac{1}{\sqrt{2\nu t + k}}. \tag{38}$$

The RHDE density ρ_{de} is obtained as

$$\rho_{de} = \frac{3c^2}{8\pi\left[\pi\delta\left(2\nu t + k\right)^2 + \left(2\nu t + k\right)\right]}. \tag{39}$$

The deceleration parameter q is calculated as

$$q = -1 + \frac{\nu}{\sqrt{2\nu t + k}}. \tag{40}$$

The shear scalar σ is obtained as

$$\sigma = \frac{K}{3exp\left(\frac{3}{\nu}\sqrt{2\nu t + k}\right)}. \tag{41}$$

The displacement field vector β is obtained from Eq. (10) as

$$\frac{3}{2}\beta\dot{\beta} + \frac{9}{2}\beta^2 H = 0. \tag{42}$$

Using Eq. (38) in Eq. (42), we get the expression of β as

$$\beta = \frac{\beta_0}{exp\left(\frac{3}{\nu}\sqrt{2\nu t + k}\right)}, \tag{43}$$

where β_0 is an integrating constant.

4. Non-interacting Model

The energy conservation equation for DM is

$$\dot{\rho}_m + 3H\rho_m = 9H^2\zeta. \tag{44}$$

The energy conservation equation for RHDE is

$$\dot{\rho}_{de} + 3H\left(1 + \omega_{de}\right)\rho_{de} = 0. \tag{45}$$

Using the expressions of H and ρ_{de} in Eq. (45), we get the expression of EOS parameter ω_{de} as

$$\omega_{de} = -1 + \frac{2\nu}{3}\sqrt{2\nu t + k}\left[\frac{2\pi\delta\left(2\nu t + k\right) + 1}{\pi\delta\left(2\nu t + k\right)^2 + \left(2\nu t + k\right)}\right], \tag{46}$$

$\omega_{de} > -1$ as observed from Fig. 3. Thus, our non-interacting model behaves like a quintessence DE.
The pressure of RHDE p_{de} is obtained as

$$p_{de} = \omega_{de}\rho_{de} = \frac{3c^2}{8\pi\left[\pi\delta\left(2\nu t + k\right)^2 + \left(2\nu t + k\right)\right]} \times \left\{-1 + \frac{2\nu}{3}\sqrt{2\nu t + k}\left[\frac{2\pi\delta\left(2\nu t + k\right) + 1}{\pi\delta\left(2\nu t + k\right)^2 + \left(2\nu t + k\right)}\right]\right\}. \tag{47}$$

With the use of Eqs. (34), (38), (40), (41), (43) and (47) in Eq. (30), we get the expression of the coefficient of bulk viscosity ζ as

$$3H\zeta = \frac{3c^2}{8\pi\left[\pi\delta\left(2\nu t+k\right)^2+\left(2\nu t+k\right)\right]}\left\{-1+\frac{2\nu}{3}\sqrt{2\nu t+k}\left[\frac{2\pi\delta\left(2\nu t+k\right)+1}{\pi\delta\left(2\nu t+k\right)^2+\left(2\nu t+k\right)}\right]\right\} + \frac{3}{2\nu t+k}-\frac{2\nu}{\left(2\nu t+k\right)^{\frac{3}{2}}}+\frac{K^2}{9exp\left(\frac{6}{\nu}\sqrt{2\nu t+k}\right)}-\frac{1}{exp\left(\frac{2}{\nu}\sqrt{2\nu t+k}\right)}+ \frac{3\beta_0^2}{4exp\left(\frac{6}{\nu}\sqrt{2\nu t+k}\right)}. \tag{48}$$

The matter energy density ρ_m is obtained from Eq. (44), using Eqs. (38) and (48) as

$$\rho_m \times exp\left(\frac{3}{\nu}\sqrt{2\nu t+k}\right) = \int\left[exp\left(\frac{3}{\nu}\sqrt{2\nu t+k}\right)\times 9H^2\zeta\right]dt+\rho_0, \tag{49}$$

where ρ_0 is a constant of integration.
The total energy density parameter Ω is given by

$$\Omega = \frac{\rho_m+\rho_{de}}{3H^2} = \frac{\rho_m+\frac{3c^2}{8\pi\left[\pi\delta(2\nu t+k)^2+(2\nu t+k)\right]}}{\left(\frac{3}{2\nu t+k}\right)} \tag{50}$$

where ρ_m is given by Eq. (49).

4.1. Energy Conditions

The Energy conditions, i.e. Weak Energy Conditions (WEC), Dominant Energy Conditions (DEC) and Strong Energy Conditions (SEC), are respectively given by:
(i) $\rho_{de} \geq 0$;
(ii) $\rho_{de}+p_{de} \geq 0$;
(iii) $\rho_{de}+3p_{de} \geq 0$.
The left-hand sides of the energy conditions for non-interacting model based on Eqs. (39) and (47) have been plotted in Fig. 7. We found that (i) $\rho_{de} \geq 0$, (ii) $\rho_{de}+p_{de} \geq 0$, and (iii) $\rho_{de}+3p_{de} \leq 0$.

So, WEC (red line) and DEC (blue line) are satisfied, whereas SEC (green line) is violated, as shown in Fig. 7.

4.2. Correspondence between non-interacting model and quintessence scalar field model

The pressure and energy density for quintessence scalar field (in ref. Sangwan et al. [2018]) are given by

$$p_\phi = \frac{\dot{\phi}^2}{2}-V\left(\phi\right), \tag{51}$$

$$\rho_\phi = \frac{\dot{\phi}^2}{2} + V(\phi), \tag{52}$$

where ϕ is the scalar field and $V(\phi)$ is the scalar field potential.
The EOS parameter ω_ϕ is defined as

$$\omega_\phi = \frac{p_\phi}{\rho_\phi} = \frac{\dot{\phi}^2 - 2V(\phi)}{\dot{\phi}^2 + 2V(\phi)}. \tag{53}$$

Eqs. (39) and (52) together imply

$$\frac{3c^2}{8\pi\left[\pi\delta\left(2\nu t + k\right)^2 + \left(2\nu t + k\right)\right]} = \frac{\dot{\phi}^2}{2} + V(\phi) \tag{54}$$

Eqs. (46) and (53) together implies

$$\frac{\dot{\phi}^2}{2} = \left(\frac{1+\omega_{de}}{1-\omega_{de}}\right) V(\phi) \tag{55}$$

Using Eq. (55) in Eq. (54), we get the expression for the scalar field potential $V(\phi)$ as

$$V(\phi) = \left(\frac{1-\omega_{de}}{2}\right)\left\{\frac{3c^2}{8\pi\left[\pi\delta\left(2\nu t + k\right)^2 + \left(2\nu t + k\right)\right]}\right\}. \tag{56}$$

Using Eq. (56) in Eq. (55), we get the expression for the scalar field ϕ as

$$\phi = \phi_0 + \int \left(1+\omega_{de}\right)^{\frac{1}{2}}\left\{\frac{3c^2}{8\pi\left[\pi\delta\left(2\nu t + k\right)^2 + \left(2\nu t + k\right)\right]}\right\}^{\frac{1}{2}} dt, \tag{57}$$

where ϕ_0 is an integrating constant.

5. Interacting Model

The energy conservation equation for DM is

$$\dot{\rho}_m + 3H\rho_m = 9H^2\zeta + 3bH\rho_{de}. \tag{58}$$

The energy conservation equation for RHDE is

$$\dot{\rho}_{de} + 3H\left(1+\omega_{de}\right)\rho_{de} = -3bH\rho_{de}. \tag{59}$$

Using the expressions of H and ρ_{de} in Eq. (59), we get the expression for the EOS parameter ω_{de} as

$$\omega_{de} = -1 - b + \frac{2\nu}{3}\sqrt{2\nu t + k}\left[\frac{2\pi\delta\left(2\nu t + k\right) + 1}{\pi\delta\left(2\nu t + k\right)^2 + \left(2\nu t + k\right)}\right]. \tag{60}$$

$\omega_{de} < -1$ as can be seen in Fig. 3. Thus, our interacting model behaves like a phantom DE.
The pressure of RHDE p_{de} is obtained as

$$p_{de} = \omega_{de}\rho_{de} = \frac{3c^2}{8\pi\left[\pi\delta\left(2\nu t + k\right)^2 + \left(2\nu t + k\right)\right]} \times \left\{-1 - b + \frac{2\nu}{3}\sqrt{2\nu t + k}\left[\frac{2\pi\delta\left(2\nu t + k\right) + 1}{\pi\delta\left(2\nu t + k\right)^2 + \left(2\nu t + k\right)}\right]\right\}. \tag{61}$$

With the use of Eqs. (34), (38), (40), (41), (43) and (61) in Eq. (30), we get the expression for the coefficient of bulk viscosity ζ as

$$\begin{aligned} 3H\zeta = {} & \frac{3c^2}{8\pi\left[\pi\delta\left(2\nu t + k\right)^2 + \left(2\nu t + k\right)\right]}\left\{-1 - b + \frac{2\nu}{3}\sqrt{2\nu t + k}\left[\frac{2\pi\delta\left(2\nu t + k\right) + 1}{\pi\delta\left(2\nu t + k\right)^2 + \left(2\nu t + k\right)}\right]\right\} \\ & + \frac{3}{2\nu t + k} - \frac{2\nu}{\left(2\nu t + k\right)^{\frac{3}{2}}} + \frac{K^2}{9exp\left(\frac{6}{\nu}\sqrt{2\nu t + k}\right)} - \frac{1}{exp\left(\frac{2}{\nu}\sqrt{2\nu t + k}\right)} + \\ & \frac{3\beta_0^2}{4exp\left(\frac{6}{\nu}\sqrt{2\nu t + k}\right)}. \end{aligned} \tag{62}$$

The matter energy density ρ_m is obtained from Eq. (58) using Eqs. (38), (39) and (62) as

$$\begin{aligned} \rho_m \times exp\left(\frac{3}{\nu}\sqrt{2\nu t + k}\right) = {} & \\ \int\left[exp\left(\frac{3}{\nu}\sqrt{2\nu t + k}\right) \times \left(9H^2\zeta + 3bH\rho_{de}\right)\right]dt + \acute{\rho_0}, & \end{aligned} \tag{63}$$

where $\acute{\rho_0}$ is a constant of integration.
The total energy density parameter Ω is given by

$$\Omega = \frac{\rho_m + \rho_{de}}{3H^2} = \frac{\rho_m + \frac{3c^2}{8\pi\left[\pi\delta(2\nu t+k)^2+(2\nu t+k)\right]}}{\left(\frac{3}{2\nu t+k}\right)}, \tag{64}$$

where ρ_m is given by Eq. (63).

5.1. Energy Conditions

The Energy conditions i.e. Weak Energy Conditions (WEC), Dominant Energy Conditions (DEC) and Strong Energy Conditions (SEC) are respectively given by:
(i) $\rho_{de} \geq 0$;
(ii) $\rho_{de} + p_{de} \geq 0$;
(iii) $\rho_{de} + 3p_{de} \geq 0$.
The left-hand sides of the energy conditions for interacting model based on Eqs. (39) and (61) have been plotted in Fig. 8 and show that (i) $\rho_{de} \geq 0$, (ii) $\rho_{de} + p_{de} \leq 0$, and (iii) $\rho_{de} + 3p_{de} \leq 0$.
So, WEC (red line) is satisfied, whereas DEC (blue line) and SEC (green line) are violated, as shown in Fig. 8.

5.2. Correspondence between Interacting model and phantom scalar field model

The pressure and energy density for phantom scalar field (in refs. Sangwan et al. [2018], Wang et al. [2010]) are given by

$$p_\phi = -\frac{\dot{\phi}^2}{2} - V(\phi), \tag{65}$$

$$\rho_\phi = -\frac{\dot{\phi}^2}{2} + V(\phi), \tag{66}$$

where ϕ is the scalar field and $V(\phi)$ is the scalar field potential.

The EOS parameter ω_ϕ is defined as

$$\omega_\phi = \frac{p_\phi}{\rho_\phi} = \frac{\dot{\phi}^2 + 2V(\phi)}{\dot{\phi}^2 - 2V(\phi)}. \tag{67}$$

Eqs. (39) and (66) together imply

$$\frac{3c^2}{8\pi\left[\pi\delta(2\nu t + k)^2 + (2\nu t + k)\right]} = -\frac{\dot{\phi}^2}{2} + V(\phi). \tag{68}$$

Eqs. (60) and (67) together imply

$$\frac{\dot{\phi}^2}{2} = -\left(\frac{1+\omega_{de}}{1-\omega_{de}}\right) V(\phi). \tag{69}$$

Using Eq. (69) in Eq. (68), we get the expression for the scalar field potential $V(\phi)$ as

$$V(\phi) = \left(\frac{1-\omega_{de}}{2}\right)\left\{\frac{3c^2}{8\pi\left[\pi\delta(2\nu t + k)^2 + (2\nu t + k)\right]}\right\}. \tag{70}$$

Using Eq. (70) in Eq. (69) and then integrating, we get the expression for the scalar field ϕ as

$$\phi = \acute{\phi_0} + \int (-1-\omega_{de})^{\frac{1}{2}} \left\{ \frac{3c^2}{8\pi \left[\pi\delta \left(2\nu t + k\right)^2 + \left(2\nu t + k\right)\right]} \right\}^{\frac{1}{2}} dt, \qquad (71)$$

where $\acute{\phi_0}$ is an integrating constant.

6. Graphical Representations

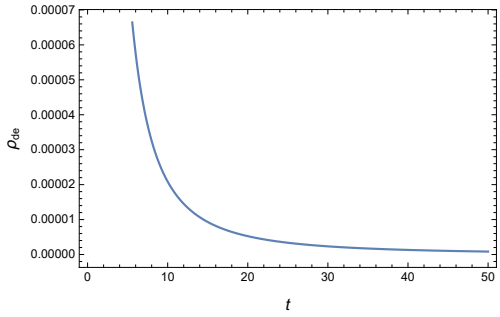

Fig. 1. Time variation of RHDE density ρ_{de}. It decreases with increasing time for $c = 1, \delta = 2, \nu = 1.5$ and $k = 0.1$. ρ_{de} approaches zero at late times, as seen in the figure.

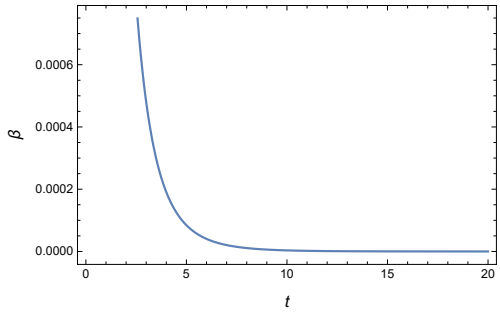

Fig. 2. Graph of β versus t, with $\beta_0 = 0.2, \nu = 1.5$ and $k = 0.1$. The graph shows that $\beta \to \infty$ when $t \to 0$, and $\beta \to 0$ when $t \to \infty$. Thus, in due course of time, the displacement field vector β loses its impact.

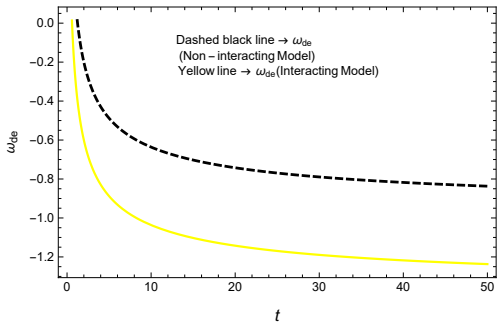

Fig. 3. The time-variation of ω_{de} for $\nu = 1.5, \delta = 2, b = 0.4$ and $k = 0.1$. From the figure, we can arrive at the conclusion that $\omega_{de} > -1$ for the non-interacting model, whereas $\omega_{de} < -1$ for the interacting model. This indicates that our non-interacting model corresponds to quintessence DE model and the interacting model corresponds to phantom DE model.

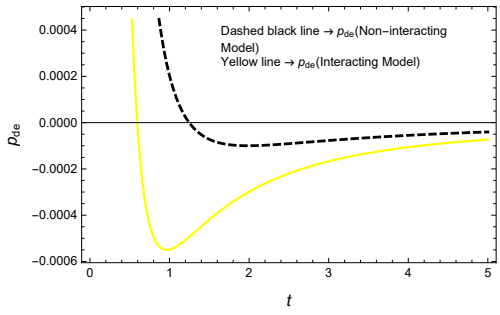

Fig. 4. The graph of p_{de} versus cosmic time t for $c = 1, \delta = 2, \nu = 1.5, b = 0.4$ and $k = 0.1$. The pressures for both non-interacting and interacting RHDE models are negative throughout the evolution of the Universe.

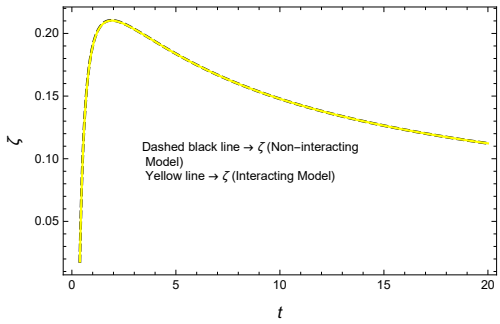

Fig. 5. The bulk viscosity ζ as a function of t with $c = 1, \delta = 2, \nu = 1.5, K = 3, \beta_0 = 0.2, b = 0.4$ and $k = 0.1$. From this figure, we can see that ζ for both non-interacting and interacting models are decreasing functions of cosmic time t and tend to have a small value as cosmic time evolves.

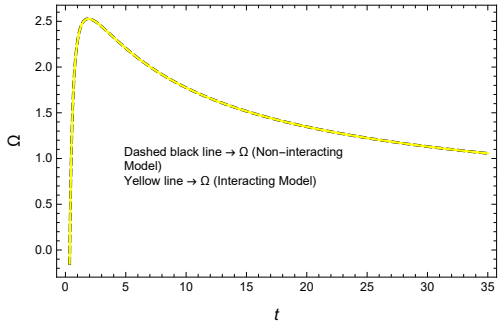

Fig. 6. The evolution of Ω w.r.to t with $c = 1, \delta = 2, \nu = 1.5, K = 3, \beta_0 = 0.2, \rho_0 = \acute{\rho_0} = 0.1, b = 0.4$ and $k = 0.1$. $\Omega \to 1$ at late times for both non-interacting and interacting models.

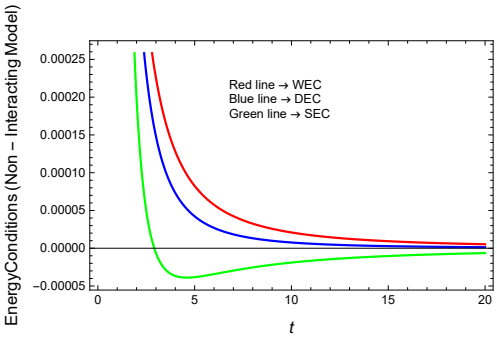

Fig. 7. The variation of Energy Conditions (non-interacting model) versus cosmic time with $c = 1, \delta = 2, \nu = 1.5$ and $k = 0.1$. The red, blue and green lines represent WEC, DEC and SEC, respectively. With the increase of cosmic time, it is found that WEC and DEC are satisfied, whereas SEC is violated.

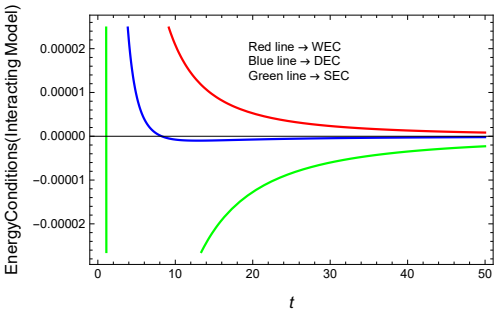

Fig. 8. The variation of Energy Conditions (interacting model) versus cosmic time with $c = 1, \delta = 2, \nu = 1.5, b = 0.4$ and $k = 0.1$. The red, blue and green lines represent WEC, DEC and SEC, respectively. With the increase of cosmic time, it is found that WEC is satisfied, whereas DEC and SEC are violated.

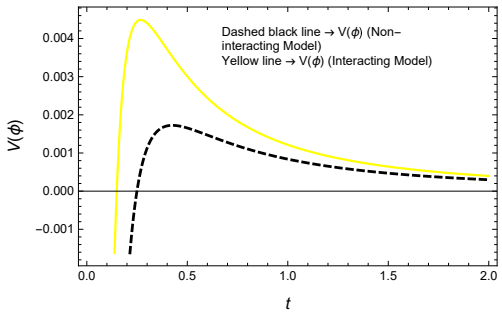

Fig. 9. The time-dependent variation of $V(\phi)$ for $c = 1, \delta = 2, \nu = 1.5, b = 0.4$ and $k = 0.1$. The scalar field potential $V(\phi)$ negatively increases from a finite value and ultimately vanishes with the evolution of the Universe for both non-interacting and interacting models.

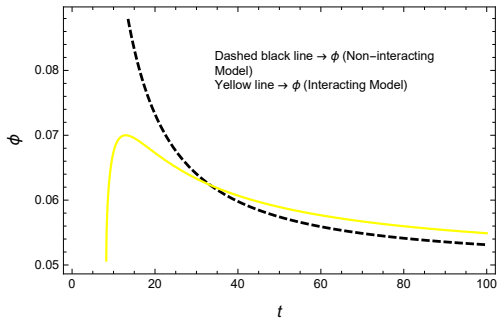

Fig. 10. The time-dependent evolution of ϕ for $c = 1, \delta = 2, b = 0.4, \nu = 1.5, \phi_0 = \acute{\phi_0} = 0.05$ and $k = 0.1$. ϕ is a decreasing function as cosmic time t evolves and ultimately tends to a small value for both non-interacting and interacting models.

7. Cosmic Jerk Parameter

It is believed that in the early Universe, the dark energy would have been too low to counteract the gravity of the matter in the Universe and, thus, the expansion was initially slow. But the dark energy dominated the matter as the Universe began to expand and grew bigger in course of time. About five to six billion years ago, DE was driving the Universe (in ref. Capozzielloo et al. [2006]). Researchers (in refs. Visser [2004], Visser [2005], Chiba and Nakamura [1998], Sahni [2002]) have suggested that the cosmic jerk is responsible for the deceleration to acceleration transition. This transition occurs for different models with a positive value of jerk parameter (j) and a negative value of deceleration parameter (q). Cosmic jerk parameter is responsible for transition from the decelerating to the accelerating phase of the Universe. The ΛCDM model has a constant jerk $j = 1$.

The mathematical expression of cosmic jerk parameter j is obtained as

$$j\left(t\right)=\frac{\dddot{a}}{aH^{3}}=\frac{3\nu^{2}}{2\nu t+k}-\frac{3\nu}{\sqrt{2\nu t+k}}+1. \tag{72}$$

From Eq. (72), we can conclude that for late times, $j\rightarrow 1$. It is also seen that the value of the cosmic jerk parameter is positive throughout the entire history of this model.

8. Statefinder Parameters

To explain the accelerating expansion of the Universe, various candidates for DE have been developed. In order to discriminate among these DE models, important parameters called Statefinder parameters, are developed by Sahni et al. [2003]. The statefinder parameters are related to the third order derivative of the average scale factor $a\left(t\right)$, and hence the depend on the metric of the space-time. The important property of the statefinder pair is that $\{r,s\}=\{1,0\}$ is a fixed-point in the $s-r$ plane for the spatially flat ΛCDM model. Hence, we have analyzed the evolutionary behavior of both the parameters r and s for the DE Universe along with ΛCDM Universe. Statefinder parameters for different DE models were studied by several researchers (Sharma and Dubey [2020], Dubey et al. [2020], Srivastava and Sharma [2020]).
The statefinder parameters are given by

$$r=\frac{\dddot{a}}{aH^{3}}=\frac{3\nu^{2}}{2\nu t+k}-\frac{3\nu}{\sqrt{2\nu t+k}}+1, \tag{73}$$

$$s=\frac{r-1}{3\left(q-\frac{1}{2}\right)}=\frac{\frac{3\nu^{2}}{2\nu t+k}-\frac{3\nu}{\sqrt{2\nu t+k}}}{3\left(\frac{-3}{2}+\frac{\nu}{\sqrt{2\nu t+k}}\right)} \tag{74}$$

When $t\rightarrow\infty$, $r\rightarrow 1$ and $s\rightarrow 0$.
So, our RHDE model corresponds to ΛCDM model at late times.

9. Anisotropy Parameter

The Anisotropy parameter A_{p} is defined as

$$A_{p}=\frac{1}{3H^{2}}\sum_{i=1}^{3}\left(H_{i}-H\right)^{2}=\left(\frac{2\nu t+k}{3}\right)\left[\frac{2K^{2}}{9}exp\left(\frac{-6}{\nu}\sqrt{2\nu t+k}\right)\right]. \tag{75}$$

From Eq. (75), we can arrive at a conclusion that $A_{p}\rightarrow 0$ as $t\rightarrow\infty$. Thus, our Universe shows isotropic behavior at the later stages.

10. Discussions and Conclusions

In this paper we have investigated the Rényi Holographic Dark Energy (RHDE) models by considering a spatially homogenous and anisotropic Bianchi type V space-time, with bulk viscosity in Lyra's manifold and with time-dependent displacement field. By considering q, the deceleration parameter as a linear function of the Hubble parameter H, the exact solutions of the field equations are obtained. In Fig. 1, we have seen that ρ_{de} is a decreasing function of t and ultimately approaches zero as $t \to \infty$. The displacement field vector β tends to zero at later ages of the Universe, which is shown in Fig. 2. The displacement field vector β plays an important role in the dynamics of the Universe. The constant displacement vector field β in Lyra geometry plays the role of the cosmological constant Λ in normal relativistic treatment (in ref. Halford [1970]). Therefore, the displacement field behaves as a candidate for dark energy. Fig. 3 shows that $\omega_{de} > -1$ with the increase of cosmic time for the non-interacting model. This depicts that our non-interacting model corresponds to quintessence DE model. For the interacting model, $\omega_{de} < -1$, as observed from Fig. 3. Thus, our interacting model behaves like a phantom DE model. The pressure p_{de} for both the non-interacting and interacting RHDE models are negative throughout the expansion of the Universe, as seen from Fig. 4. From Fig. 5, it is observed that ζ decreases as the cosmic time t evolves and ultimately tends toward a small value, which speeds up the accelerated expansion of the Universe for both non-interacting and interacting models. The total energy density parameter $\Omega \to 1$ as time increases for both non-interacting and interacting models, as seen from Fig. 6. So, our Universe becomes spatially homogeneous, isotropic and flat at later times. For the non-interacting model, WEC and DEC are satisfied, whereas SEC is violated. For the interacting model, WEC is satisfied, but DEC and SEC are violated. The violation of DEC and SEC supports the fact that the Universe is expanding at an accelerated rate, being filled with a phantom fluid (in ref. Sahoo et al. [2018]). The scalar field potential $V(\phi)$ negatively increases from a finite value and ultimately vanishes with the evolution of the Universe for both the non-interacting and interacting models. The scalar field ϕ is diminishing and ultimately tends toward a small value as cosmic time evolves for both the non-interacting and interacting models. Cosmic jerk parameter $j \to 1$ with the passage of time, and it is positive throughout the entire age of the Universe. The statefinder parameters $\{r, s\}$ correspond to ΛCDM model at late times. The anisotropy parameter $A_p \to 0$, as $t \to \infty$, which indicates that our RHDE model shows isotropic behavior throughout the evolution of the Universe. The aforesaid results indicate that our models are in good agreement with the present-day observations and establish the fact that the Universe is accelerating.

Acknowledgements

We would like to appreciate the Department of Mathematics, Gauhati University for the research supportive environment which allowed us to conduct and complete this research work. One of the authors (JB) acknowledges the financial support from UGC (NFOBC), India for doing this research work.

References

Ade P. A. R., Aghanim N., Armitage-Caplan C., Arnaud M., Ashdown M., Atrio-F., Aumont J., et al., 2013, arXiv: 1303.5076
Bennett C. L., Halpern M., Hinshaw G., Jarosik N., Kogut A., Limon M., Meyer S. S., et al., 2003, *Astrophys. J. Suppl. Ser.* 148, 1
Bhattacharjee S., 2020, arXiv: 2006.04339v1 [gr-qc]
Bolotin Y. L., Cherkaskiy V. A., Lemets O. A., Yerokhin D. A., and Zazunov L. G., 2015, arXiv: 1502.00811 [gr-qc]
Caldwell R. R., Kamionkowski M., and Weinberg N. N., 2003, *Phys. Rev. Lett.* 91, 071301
Capozziello S., Nojiri S., and Odintsov S. D., 2006, *Phys. Lett. B.* 632, 597-604
Carroll S. M., Hoffman M., and Trodden M., 2003, arXiv: astro-ph/0301273v2
Chiba T., 2002, arXiv: astro-ph/0206298v2
Chiba T., and Nakamura T., 1998, *Prog. Theor. Phys.* 100, 1077
Cohen A. G., Kaplan D. B., and Nelson A. E., 1999, *Phys. Rev. Lett.* 82 (25), 4971
Divya Prasanthi U. Y., and Aditya Y., 2020, *Results in Phys.* 17, 103101
Dubey V. C., Mishra A. K., and Sharma U. K., 2020, arXiv:2003.07883v1 [gr-qc]
Gilliland R. L., et al., 1998, *Astron. J.* 116, 1009-1038
Halford W. D., 1970, *Australian. J. Phys.* 23, 863
Hooft G. 't, 1993, arXiv: gr-qc/9310026
Kamenshchik A. Y., Moschella U., and Pasquier V., 2001, *Phys. Lett. B* 511, 265-268
Kandalkar S. P., and Samdurkar S., 2015, *Bulg. J. Phys.* 42, 42-52
Li M., 2004, *Phys. Lett. B* 603, 1
Lyra G., 1951, *Math Z* 54, 52
Meng X., and Ma Z., 2012, *Eur. Phys. J. C* 72, 2053
Misner C. W., 1968, *Astrophys. J.* 151, 431–457
Moradpour H., Moosavi S. A., Lobo I. P., Morais Graça J. P., Jawad A., and Salako I. G., 2018, *Eur. Phys. J. C* 78, 829
Overduin J. M., and Cooperstock F. I., 1998, *Phys. Rev. D* 58, 043506
Padmanabhan T., and Chitre S. M., 1987, *Phys. Lett. A.* 120, 433–436
Page L., Nolta M. R., Barnes C., Bennett C. L., Halpern M., Hinshaw G., Jarosik N., et al., 2003, *Astrophys. J. Suppl. Ser.* 148, 233-241
Perlmutter S., Aldering G., Della Valle M., Deustua S., Ellis R. S., Fabbro S., Fruchter A., et al., 1998, *Nature* 391, 51-54
Pradhan A., and Pandey H. R., 2003, arXiv: gr-qc/0307038v1
Pradhan A., Pandey P., Jotania K., and Yadav M. K., 2007, *Int. J. Theor. Phys.* 46, 2774-2787
Pradhan A., Yadav V. K., and Chakrabarty I., 2001, *Int. J. Mod. Phys. D* 10 (3), 339-349
Riess A. G., Filippenko A. V., Challis P., Clocchiatti A., Diercks A., Garnavich P. M., Gilliland R. L., et al., 1998, *Astron. J.* 116, 1009-1038
Saha B., and Rikhvitsky V., 2006, *Physica D* 219, 168-176
Sahni V., 2002, arXiv: astro-ph/0211084
Sahni V., Saini T. D., Starobinsky A. A., and Alam U., 2003, *JETP Lett.* 77 (5), 201-206
Sami M., and Padmanabhan T., 2003, *Phys. Rev. D* 67, 083509
Sangwan A., Mukherjee A., and Jassal H. K., 2018, *JCAP* 01, 018
Sahoo P. K., Moraes P. H. R. S., Sahoo P., and Ribeiro G., 2018, *Int. J. Mod. Phys. D* 27, 1950004
Sen D. K., 1957, *Z. Physik* 149, 311
Sen D. K., and Dunn K. A., 1971, *J. Math. Phys.* 12, 578
Sharma U. K., and Dubey V. C., 2020, arXiv: 2001.02368v1 [gr-qc]
Sharma U. K., and Dubey V. C., 2020, *New Astronomy* 80, 101419
Singh C. P., 2008, *Pramana J. Phys.* 71, 33-48
Singh C. P., and Srivastava M., 2018, *Eur. Phys. J. C* 78, 190
Singh T., and Chaubey R., 2007, *Pramana J. Phys.* 68, 721-734
Spergel D. N., Verde L., Peiris H. V., Komatsu E., Nolta M. R., Bennett C. L., Halpern M., et al., 2003, *Astrophys. J. Suppl. Ser.* 148, 175-194
Srivastava V., and Sharma U. K., 2020, *New Astronomy* 78, 101380
Susskind L., 1995, *J. Math. Phys.* 36, 6377
Tegmark M., et al., 2004, *Phys. Rev. D* 69, 103501
Tiwari R. K., Beesham A., and Shukla B., 2018, *Int. J. Geom. Meth. Mod. Phys.* 15, 1850115
Tiwari R. K., Beesham A., and Shukla B. K., 2017, *Eur. Phys. J. Plus* 132, 126
Tiwari R. K., Beesham A., and Shukla B. K., 2017, *Eur. Phys. J. Plus* 132, 20

Tiwari R. K., Beesham A., and Shukla B. K., 2016, *Eur. Phys. J. Plus* 131, 447
Visser M., 2004, *Class. Quant. Grav.* 21, 2603-2616
Visser M., 2005, *Gen. Relativ. Gravit.* 37, 1541
Wang W. F., Shui Z. W, and Tang B., 2010, *Chin. Phys. B* 19, 11
Wei H., and Cai R. G., 2009, *Eur. Phys. J. C* 59, 99-105
Weinberg S., 1989, *Rev. Mod. Phys.* 61, 1
Weinberg S., 1971, *Astrophys. J.* 168, 175
Weinberg S., 1972, *Gravitation and Cosmology* Wiley and Sons, New York
Weyl H., 1918, *Ann. Phys. Leipzig* 54, 117